# Non-linear Finite Element Analysis of Deep Beams

Analyse non-linéaire par éléments finis de poutres de petite portée

Nichtlineare Finite-Elemente-Berechnung von hohen Trägern

**JUNICHIRO NIWA**
Graduate Student
University of Tokyo
Tokyo, Japan

**KOHICHI MAEKAWA**
Graduate Student
University of Tokyo
Tokyo, Japan

**HAJIME OKAMURA**
Associate Professor
University of Tokyo
Tokyo, Japan

## SUMMARY
A non-linear finite element method of analysis was applied to predict the behavior of reinforced concrete deep beams. The behavior of concrete including strain softening tendency and anisotropy was modelled by the total strain theory and combined with non-linear analysis. The analytical results were compared with the experimental results. The techniques for the non-linear method of analysis and the capability to predict the behavior of deep beams were investigated.

## RÉSUMÉ
Le comportement non-linéaire de poutres en béton armé de petite portée est analysé par éléments finis. Le comportement du béton, comprenant l'anisotropie et le "strain-softening", est simulé par la théorie de la déformation totale combinée à l'analyse non-linéaire. Les résultats analytiques furent comparés aux résultats expérimentaux. Les techniques d'analyse non-linéaire et la capacité de prédiction du comportement de poutres à petite portée sont analysées.

## ZUSAMMENFASSUNG
Eine nichtlineare Finite-Elemente-Methode wurde auf die Berechnung von hohen Trägern aus Stahlbeton angewandt. Das Verhalten mit Einschluss von Steifigkeitsabnahme und Anisotropie wurde mit einer nichtlinearen Berechnung kombiniert. Theorie und Experiment an hohen Trägern wurden verglichen.

## 1. INTRODUCTION

The behavior of reinforced concrete structures under applied loads
is complex due to numerous internal load paths. Such load paths
vary a great deal due to the distribution of stiffness in the
structure, and that variation in stiffness arises from variable
pattern and sequence of crack occurrence and plastification of
materials. On the other hand the whole picture of the
constitutive law of concrete is not yet apparent particularly when
the combination of applied stresses changes as they are increased.
The various factors influencing the behavior of reinforced
concrete structures are interlaced and therefore, any devised
methods of analysis need be scrutinized in the lights of
experimental observations [1].

A finite element method of analysis with a few techniques to
overcome the difficulties characteristic to nonlinearlity was
presented to predict the behavior of reinforced concrete deep
beams and the analytical results were compared with the
experimental results specially tested for this purpose.

## 2. NUMERICAL METHOD

In the analysis step iterative procedure for non-linear finite
element method was used. In applying the analysis to deep beams,
enforced displacements were imposed because of the easier
evaluation of the ultimate strength. The general flow of the main
routine is as shown in Fig.1.

At the first iteration of each step, the equivalent nodal forces,
which appear when constraint displacements are applied to the
structures, are calculated using the updated stiffness matrix in
the preceding step. During iterative routine, the stiffness
matrix was formed at each iteration. The increments of nodal
displacements are then calculated.

$$u = K^{-1} \Delta F \tag{1}$$

$$\Delta F = F - \iiint B^T \sigma \, dv \tag{2}$$

K : global stiffness matrix , F : equivalent nodal force
F : total external nodal forces, F=0 in this analysis
B : strain displacement matrix , $\sigma$ : stresses

In each iteration, the unbalanced forces are calculated by
equation 2. If unbalanced forces are not as small as required,
the next incremental displacements are calculated by setting the
equivalent nodal forces as the unbalanced forces. When the value
of unbalanced force differs from that of previous iterative
routine significantly or the direction of the force changes, the
nodal force increment for correction is made one half the
corresponding unbalanced force. The selection of one half is
arbitrary, but by this procedure, the risk of divergence or a
great leap beyond equlibrium points was avoided to some extent.

Enforced Displacement $U_2 = U_2 + {}_\Delta U_2$

Equivalent Nodal Force ${}_\Delta F_1 = -K_{12\Delta} U_2$

Stiffness Matrix $K = K(\varepsilon)$

Displacement $\quad {}_\Delta U_1 = K_{11\Delta}^{-1} F_1$
$U_1 = U_1 + {}_\Delta U_1$

Strain $\quad \varepsilon = \varepsilon + B_\Delta U$

Stress $\quad \sigma = \sigma(\varepsilon)$

Unbalanced Nodal Force $\quad {}_{\Delta\Delta} F_1 = -\iiint B^T \sigma dv$

$\| {}_{\Delta\Delta} F_1 \| < \delta$

No

Yes

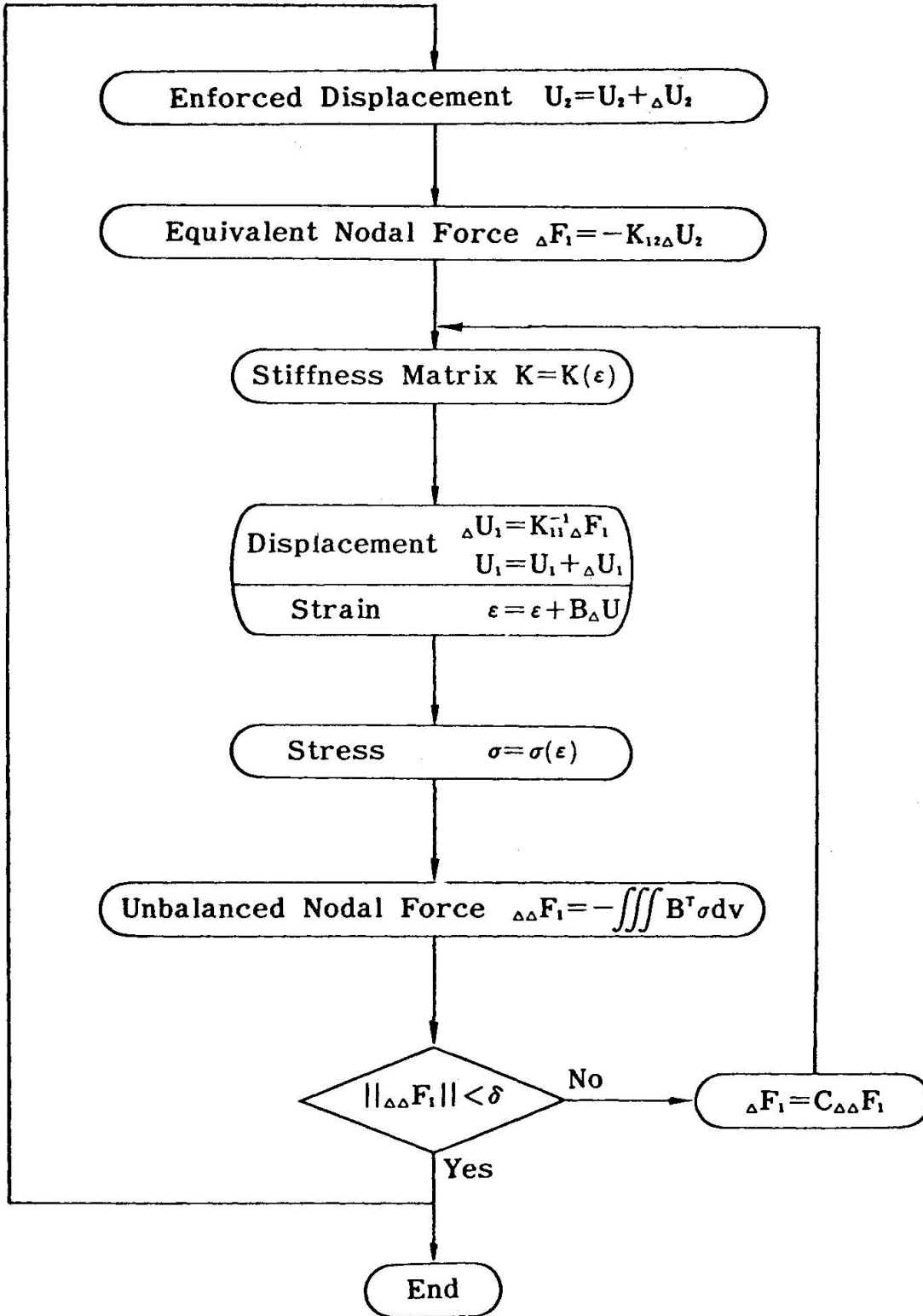${}_\Delta F_1 = C_{\Delta\Delta} F_1$

End

Fig. 1　General Flowchart of Non-linear Iterative Routine

## 3. CONSTITUTIVE EQUATIONS OF CONCRETE

### 3.1 Stress strain relationship of concrete

There exist two families of constitutive formulations according to
the method of stress evaluation, namely differential and total
strain formulation. The former evaluates stresses by integrating
stress increment at each step. The total strain formulation
calculates stresses by total strains and constitutive equations
which contain invariants with regard to coordinate transformations
as parameters. In the analysis the total strain formulation was
used for evaluating stresses for the following reasons.
(a) Strain softening tendency under multiaxial stress states is
easily modeled.
(b) No accumulation of errors in estimating the stresses occurs so
that the step size can be set relatively large.
(c) Experimental data are directly used for making the
constitutive equations.

The constitutive law used for the analysis of deep beams is two
dimentional, and the following scalar values named equivalent
stress and equivalent strain which are indicated by stress and
strain invariants with regard to coordinate transformations are
defined.

$$s = s(\sigma_{ij}) = s(\sigma_1, \sigma_2) = \sqrt{\left(\frac{\sigma_1 + \sigma_2}{2.32fc}\right)^2 + \left(\frac{\sigma_1 - \sigma_2}{1.108fc}\right)^2} \qquad (3)$$

$$e = e(\varepsilon_{ij}) = e(\varepsilon_1, \varepsilon_2) = \sqrt{\left(\frac{\varepsilon_1 + \varepsilon_2}{9.6 \times 10^{-4}}\right)^2 + \left(\frac{\varepsilon_1 - \varepsilon_2}{6.2 \times 10^{-4}}\right)^2} \bigg/ \sqrt{fc} \qquad (4)$$

where s : equivalent stress, e : equivalent strain
fc : uniaxial compressive strength, assumed as 90% of the
cylinder strength [2]
$\sigma_1$ $\sigma_2$ : principal stresses ( $\sigma_1 > \sigma_2$ ), $\varepsilon_1$ $\varepsilon_2$ : principal strains

These two invariants represent the degree of stress and strain
level respectively, and are introduced in order to allow the
actual biaxial stress-strain curves to be expressed in an
one-to-one relationship as in the case of uniaxial conditions, so
that a family of uniaxial concepts of stress-strain relationships
is to be used. This equation was determined by a least squares
fit of biquadratic polynomial from the reported experimental data
[2,3,4,5].

$$s = f(e) \qquad (5)$$

$$= 1.042 \ e - 2.083 \ e + 0.42 \ e + 2.0 \ e \quad : e < e2$$

$$= -0.25 \ e + 1.25 \quad : e > e2$$

The relationship of each stress and strain components in the local
coordinate system whose axes coincide with the principal stress
axes is developed, in consideration of anisotropic characreristics
of concrete due to microcracking and void formation. These
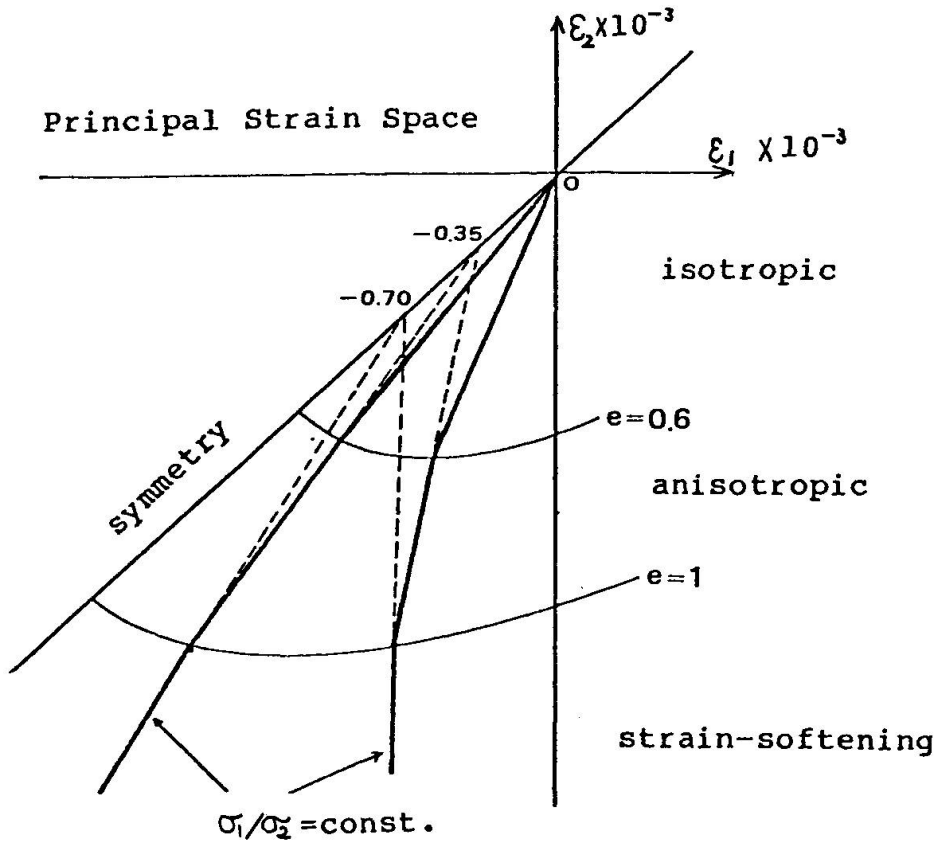characteristics of concrete are dependent on the strain level, and

Fig. 2   Proportional Loading Pathes on Principal Strain Surtace

the relationship of two principal strains under constant principal stress ratio is modeled as tri-linear one as shown in Fig.2. The relation is developed based on the reported experimental data [2], [3],[4].

In the low level of strain, concrete can be assumed an isotropic material [5] and the relation of two principal values, stresses and strains, is reasonablely assumed as the one for elastic materials.

$$p = (q + \nu)/(1 + \nu*q)$$                                             (6)

where p : stress ratio = $\sigma_1/\sigma_2$ ,q : strain ratio = $\varepsilon_1/\varepsilon_2$
      $\nu$ : Poisson's ratio

On increasing the strain to a high level, a stage is reached where the microcracking between aggregates and mortar starts to propagate and the anisotropic behavior appears gradually. This boundary between the isotropic and the anisotropic is assumed to depend on the value of the equivalent strain, and is assumed as 0.6 in the calculation (see Fig.2). After this stage the slope of the line which shows the relationship of the two principal strains is changed to express the anisotropic behavior of concrete. When the strain-softening level is attained (e=1), the effect of

anisotropic behavior and drastic void formation becomes significant, and the slope is changed again.

When two principal strains are given, the corresponding strain ratio at the isotropic stage is obtained by using the tri-linear relation as shown in Fig.2. Then, the stress ratio is calculated by equation 6. Using this stress ratio and the equivalent stress, which can be calculated by equation 5, each principal stress is calculated by using equation 3.
s.2 Cracking

In non-linear finite element method of analysis, there are two methods for representing the behavior of cracked concrete; discrete crack and smeared crack model. The former simulates a crack by releasing the connection of each element. The latter represents a crack by modifying the constitutive equations. The smeared crack model can simulate the total responses of structural systems in which crackings occur, and was used for the analysis of deep beams.

Criterion of cracking is determined by stresses, and cracking is defined to occur when the principal stresses make the following crack index equal to unity.

$$Ci = (\sigma_1/ft) - \sqrt[3]{(1 + \sigma_2/fc)} : \text{under compression-tension}$$
$$= (\sigma_1/ft) - 1 : \text{under biaxial tention} \qquad (7)$$

where ft : uniaxial tensile strength

The orientation of crack is considered to be normal to the major principal stress, and the stress component normal to a crack is reduced to zero. The condition, where the crack index is zero, represents the failure envelope at compression-tension and tension-tension stress states. When the value of crack index is between zero and one, stress normal to the direction of a crack is maintained constant although the stress calculated by the above mentioned method exceeds the value corresponding to zero of crack index.

Shear transfer across the crack is simply simulated by changing the shear stiffness along the crack as shown in equation 10. Calculations were made by zero stiffness in general and half of the uncracked stiffness in some case. When the strain normal to the crack is compressive, the crack is closed and the condition is assumed to be the same as that of uncracked concrete. If concrete at an evaluation point has previous experiences of cracking, the stress component normal to the crack is calculated and the crack is assumed to open again when the stress is tensile.


## 3.2 Stiffness of iterative calculation

In the non-linear iterative procedures a stiffness for each evaluation point is necessary. The stiffness matrix is formed by superposing the isotropic stiffnesses of uncracked concrete and

the anisotropic stiffnesses of cracked one. The assumption of
quivalent stress-strain relationship permits the evaluation of
incremental elastic moduli as in equation 8.

$$E = E0 \ \frac{ds/de}{ds/de \, | \, e=0}$$                    (8)

where E0 is the initial tangent stiffness moduli

With the tangent moduli and effective Poisson's ratio, the
isotropic tangent stiffness matrix of uncracked concrete is
obtained by equation 9. The anisotropic tangent stiffness of
cracked concrete is written in equation 10, using the tangent
moduli parallel to crack direction. The effective Poisson's ratio
is also assumed as in equation 12 in consideration of the
equivalent strain level.

$$\frac{E}{1-\nu^2} \begin{bmatrix} 1 & \nu & 0 \\ \nu & 1 & 0 \\ 0 & 0 & \frac{1-\nu}{2} \end{bmatrix}$$                    (9)

$$\begin{bmatrix} 0 & 0 & 0 \\ 0 & E & 0 \\ 0 & 0 & \alpha G \end{bmatrix}$$                    (10)

where $\alpha = 0$ or $0.5$,    $G = E/(2(1+\nu))$    (11)

$$\nu = 0.2 \qquad\qquad e < e1$$
$$= 1.75 \ e - 0.85 \qquad e1 < e < e2 \qquad (12)$$
$$= 0.9 \qquad\qquad e > e2$$

A lower limit is set for the possitive tangent stiffness, because
the global tangent stiffness matrix becomes numerically unstable
when diagonal terms approach zero. One hundredth of the initial
tangent stiffness was used for the lower limit, after some trial
calculations were executed.

## 4. APPLICATION TO THE ANALYSIS OF DEEP BEAMS

Reinforced concrete deep beam is one of the problems which need the help of a suitable non-linear finite element method of analysis for understanding the behavior. The applicability of the analytical method to deep beams is investigated. Deep beams used in the comparison with the analytical results were particularly tested for this purpose. The characteristics of eight specimens are shown in Table 1. The parameters such as concrete strength ( 13 MPa - 67 MPa ), reinforcement ratio ( 3 % - 6 % ), shear span ( 150 mm - 200 mm ) and height of beam ( 300 mm - 600 mm ) are widely and systematically varied. To ensure the anchorage, main reinforcing bars were bent up as shown in Fig.4. No shear reinforcement is used.
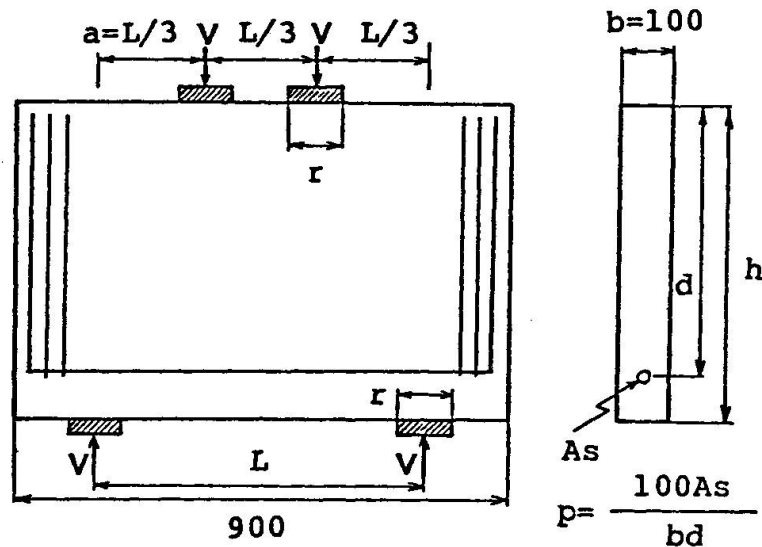


Fig. 4   Deep Beam Specimens Tested

Table 1   Characteristics of Deep Beam Specimens

| Beam | a(mm) | d(mm) | a/d | r(mm) | h(mm) | p(%) | fy(MPa) | fc'(MPa) |
|------|-------|-------|------|-------|-------|------|---------|----------|
| T1 | 200 | 228 | 0.88 | 140 | 300 | 6.0 | 364 | 35.8 |
| T2 | 200 | 507 | 0.39 | 100 | 600 | 3.0 | 389 | 54.7 |
| T3 | 200 | 228 | 0.88 | 100 | 300 | 3.0 | 364 | 13.1 |
| T4 | 150 | 507 | 0.30 | 140 | 600 | 3.0 | 389 | 13.1 |
| T5 | 200 | 507 | 0.39 | 140 | 600 | 6.0 | 389 | 66.6 |
| T6 | 150 | 507 | 0.30 | 100 | 600 | 6.0 | 389 | 35.8 |
| T7 | 150 | 228 | 0.66 | 100 | 300 | 6.0 | 364 | 59.9 |
| T8 | 150 | 228 | 0.66 | 140 | 300 | 3.0 | 364 | 58.8 |

Considering the flow of stresses in the beam, a finite number of skew quadrilateral elements as shown in Fig.5 were used for the analysis of plane stress conditions. The same topological shapes and number of elements were used for all the eight beams.

The assumption of the plane stress is considered to be reasonable for most portions of the beam. But, concrete near the bearing plate is obviously stressed triaxially and the effect on the behavior of the beam is not negligibly small, especially in the concrete mainly stressed in compression by bending moment. Therefore, five elements hatched in Fig.5 were to have an apparent higher compressive strength 1.8 times that for other elements. However, the concrete strength for the element at the span center was made normal, so that the increase of concrete strength

in triaxial compression zone might
not affect the flexure dominant
strength of the beam.

Eight nodes isoparametric elements
were used taking into account that
the strain distribution in the beam
is more or less linear.  Two by two
stress evaluation points, or Gauss
points, were arranged in each
element.  This number of Gauss
points may ordinarily be sufficient.
However, five by five Gauss points
were arranged in four elements where
strains have the possibility of                    Fig. 5   Idealization of
changing from a very small magnitude                        Finite Elements
to softening level within the element.
The elements are marked with character 5 in Fig.5.  For this kind
of element, two by two points were insufficient for the evaluation
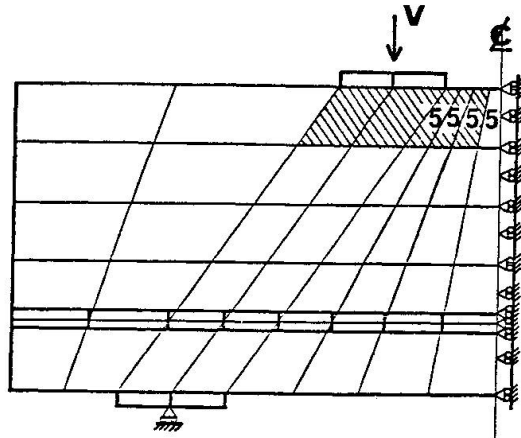of stresses.

Totally, 40 concrete and 12 steel elements with 174 nodes and 292
Gauss points were used.  The CPU time to calculate ten steps with
two iterations in each step was about 70 seconds using a HITAC
M-200H system at the computer center of University of Tokyo, and
the computation fee for one case was about 500 yen ( $ 2.50 ).

A perfect bond of steel and concrete was assumed at the selected
nodes and no bond was assumed in other places.  In order to effect
this particular bond behavior, the nodes of steel elements were
connected to the nodes of concrete elements that were located at
the same level as the center of steel elements.

## 5.  EVALUATION OF THE ANALYTICAL RESULTS

### 5.1. Failure Mode and Ultimate Load

Failure modes predicted by the analysis, when the shear stiffness
along the cracks is assumed to be zero, otherwize shear transfer
across the cracks is ignored, are classified into three types :
(a) diagonal compression failure of concrete above the support,
(b) flexural compression failure of concrete at the section in the
center of the span, and (c) flexural failure due to yielding of
main reinforcing steel.

Four beams classified in diagonal compression failure have small
shear span-depth ratios equal to 0.30 and 0.39 .  Analytical
results of these cases showed that the principal compressive
stresses in the elements above the support were maximum among all
elements.  Stresses increased with applied enforced displacements
and the elements gradually became plastic and softened.  As a
result, stress redistribution occurred.  Stresses in adjacent
elements increased and stress distribution became more uniform and
the load carrying capacity of the beam became the maximum.  When
strains of softened elements above the support became very large

and stresses decreased extremely, stresses of other elements that
had not yet been plastic began to decrease.

In the experiment, four beams, T2,T4,T5 and T6, which belonged to
case (a) indeed failed in diagonal compression above the support.
Observed failed portions of the specimen T5 is shown by shadow in
Fig.6(a). Predicted results are very similar to observed results
in failure mode and failed portions.

Analytical results of case (b) showed that the most critical
stress state existed in the element of the top surface and at the
span center where the moment is maximum. With an increase of
applied displacement, stresses of the element increased and the
element became plastic and softened. On the other hand, adjacent
elements of top surface, which have the higher strength, nor the
elements above the support did not become plastic.

In the experiments, three beams, T1,T3 and T7, which belonged to
case (b), did not fail at the sections in the maximum moment
region. Observed failed portions of the specimen T7 is shown by
shadow in Fig.6(b). When cracks possessing an angle steeper than
already existing diagonal cracks developed towards the edges of
the bearing plate, slip occurred along this crack and the beam
failed. This type of slip failure mode was not predicted by this
analysis. This was considered to be due to the ignorance of the
shear transfer. Therefore, trial calculations were executed on
the assumption that the shear stiffness along the crack is made
half of the uncracked one( $\alpha$ = 0.5 in equation 11 ). The results
of calculations for T1 and T7 conformed that the secondary crack
occurred in the point above the support at lower load than the
ultimate load predicted by the analysis without shear transfer.
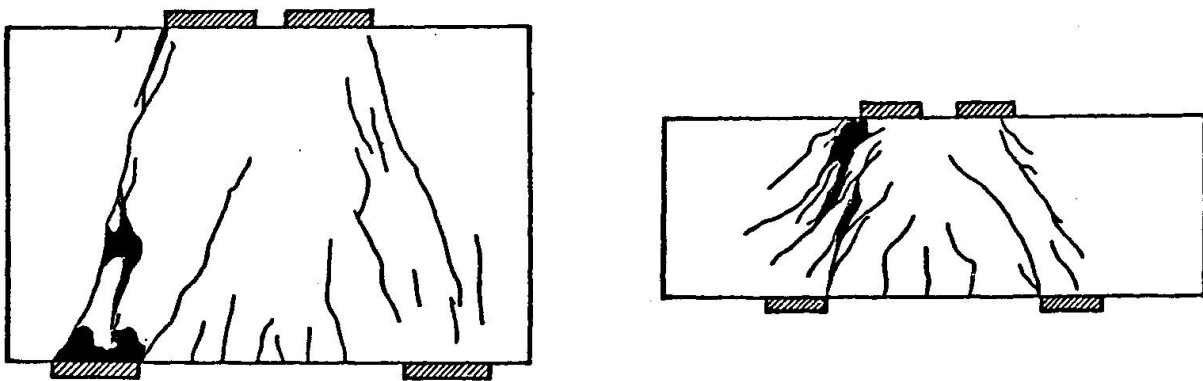


(a) T5, predicted to be failed          (b) T7, predicted to be failed
    in diagonal compression                 in flexural compression

Fig. 6    Crack Formation and Failed Portions

This will suggest that the proper modeling for shear transfer is extremely important for the analysis of this type of beams.

Results of analysis of case (c) showed that the beam failed in flexural mode governed by yielding of steel. The observed failure of T8, which belonged to case (c), was also in flexural mode.

Predicted failure modes and loads are given in Table 2 in comparison with the experimental values. The average ratio of the experimental ultimate load to the analytical one is 0.96 with the coefficient of variation of 0.18.

Table 2  Failure Mode and Ultimate Load

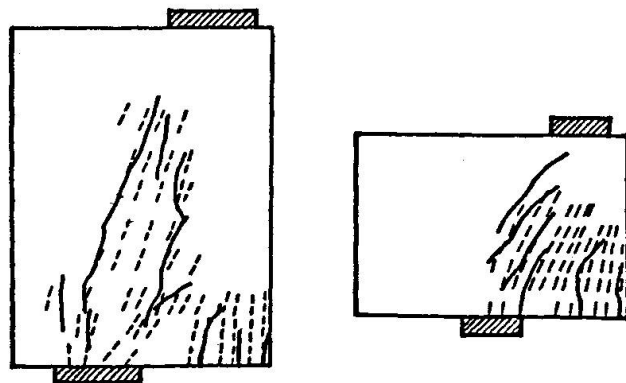| Beam | Failure Mode expt. | Failure Mode anal. | Ultimate Load (KN) expt. | Ultimate Load (KN) anal. | Ultimate Load (KN) expt./anal. |
|------|------|------|------|------|------|
| T1 | SL | FC | 629 | 506 | 1.24 |
| T2 | DC | DC | 1028 | 1373 | 0.75 |
| T3 | SL | FC | 228 | 235 | 0.97 |
| T4 | DC | DC | 425 | 484 | 0.88 |
| T5 | DC | DC | 1763 | 1930 | 0.91 |
| T6 | DC | DC | 1155 | 996 | 1.16 |
| T7 | SL | FC | 892 | 1221 | 0.73 |
| T8 | FT | FT | 941 | 888 | 1.06 |

DC:Diagonal
   Compression
SL:Slip
FC:Flexural
   Compression
FT:Flexural
   Tension

## 5.2 Diagonal Cracking

According to the analysis two types of diagonal cracking mode was recognized.  Four specimens, which had small a/d and belonged to case (a), and the rest, which had large a/d and belonged to case (b), showed different tendencies.

The analysis of small a/d specimens predicted that diagonal cracks developed dominantly while the development of flexural cracks was limited.  On the other hand, in the analysis of large a/d specimens, diagonal cracks were distributed and developed uniformly in larger areas. Further, flexural cracks developed extensively.  In Fig.7, predicted crack development of T5 as an example of small a/d specimens and T7 as an example of large a/d specimens are shown by broken lines.  The load level in these figures is about 70% of analytical maximum load.

In the experiments, development of dominant and long diagonal cracks were indeed characteristic of all small a/d beams and distributed diagonal cracks characterized large a/d beams. In Fig. 7,

(a) T5                    (b) T7

Fig. 7  Predicted and Observed
        Crack Pattern

development of observed cracks are superposed by bold lines. In
both small and large a/d beams, positions of predicted and
observed diagonal cracks are not necessarily coincident to each
other. However, in consideration of the fact that crack
evaluation points are discrete, the locations of cracks may be
said to be similar. Moreover, directions of diagonal cracks are
similar both in the prediction and in the observation. Therefore,
it is deduced that this analysis can predict the actual
behaviors reasonably accurately with regard to positions and
directions of diagonal  crack development for  all the specimens.

## 5.3. Displacement and Strains of Concrete

The displacement of beam was satisfactorily predicted by the
analysis.  Fig.8 shows an example of the relationship between
applied shear forces and the relative displacements of T5 specimen
with the experimental values.

Fig.9 shows an example of the relationship between applied shear
forces and the compressive principal strains of concrete just
above the support. The tested values were obtained from the
gauges attached to the surfaces of specimen T5. Fig.10 shows
examples of strain distributions of Gauss points located at the
same level of the concrete strut. These figures clearly show that
strains of concrete and the displacement can be satisfactorily
predicted by the analysis for the beams failed in diagonal
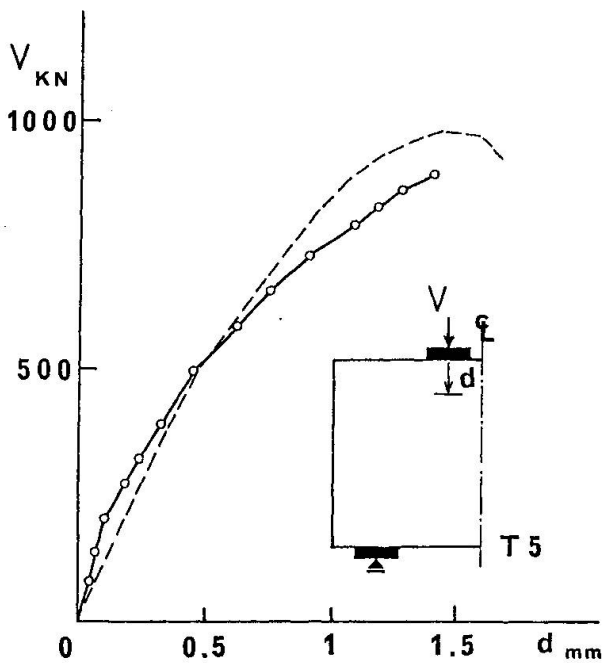compression mode.
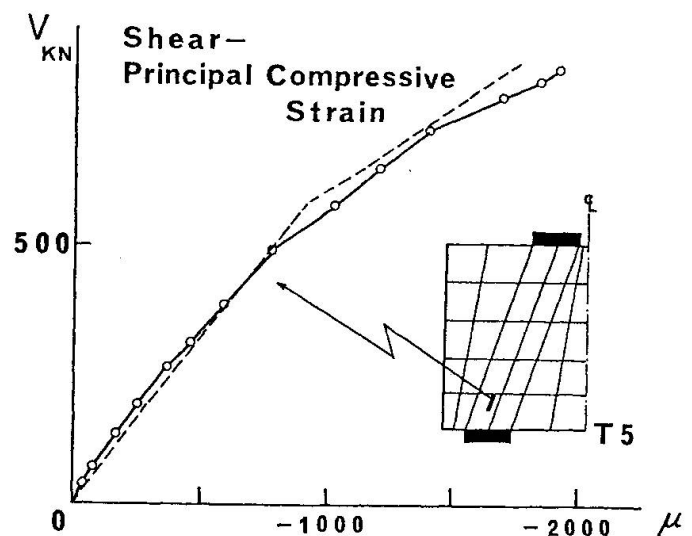
Fig.8    Shear-Displacement

Fig.9 Shear-Compressive
Strain

## 5.4. Evaluation of the Finite Element Analysis

Three types of failure mode were predicted by this analysis.
In case (a), that is, diagonal compression failure mode of concrete above the support, the observed diagonal cracking pattern, stress distribution and failure mode were predicted reasonably accurately. Therefore, it is admitted that this analysis can estimate the actual behavior, on the whole, of this type of failure mode.



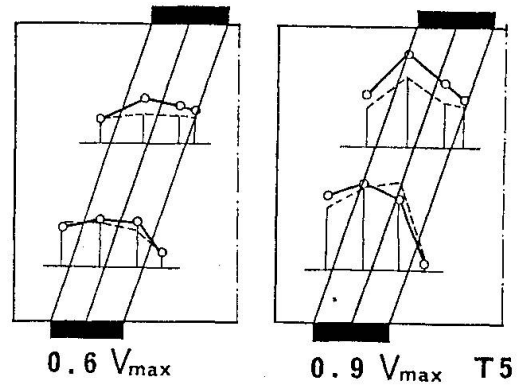**0.6 $V_{max}$**        **0.9 $V_{max}$   T5**

Fig.10    Strain Distribution in Concrete Strut

Secondly, in case (b), that is, flexural compression failure mode of concrete at the center span, the observed diagonal cracking pattern was predicted reasonably accurately but the variation of crack directions with load and failure mode could not be predicted by ignoring the shear stiffness along inclined cracks. Without shear transfer along the inclined crack surfaces, the stress condition in diagonal concrete struts bordered with diagonal cracks is almost uniaxial compression. When the shear stiffness is considered, there are additional shear stresses along the cracks and the resulting stress condition is severer ( provided the existing compressive stress remains constant ). Hence, the additional shear stress at crack surface results in undesirable stress condition in the diagonal concrete struts. The estimation of shear transfer along cracks is an important problem in order to predict the slip failure mode along a new surface inclined to the earlier cracks.

In case (c), that is, yielding of main reinforcement, the observed behaviors were adequately predicted.

## 6. CONCLUDING REMARKS

The behavior of reinforced concrete deep beams under increasing load was analyzed by a non-linear finite element method of analysis and the results were compared with experimental observations. For the loading tests of reinforced concrete deep beams the influencial parameters such as geometrical configuration, concrete strength and reinforcement ratio were varied so that various load carrying mechanisms can be observed. The bi-axial stress-strain relationship of concrete was expressed by a relation between stress and strain invariants developed herein. The following remarks appear to be relevant regarding the

techniques for non-linear method of analysis and capability of behavior prediction of deep beams.

(1). A step-iterative procedure of imposed displacement analysis was effective for solution of the behavior of structures where the portions were in strain softening region.

(2). The three failure modes observed on deep beam test specimens were, (a) crushing near the bottom of diagonal concrete struts, (b) slip along diagonal crack and (c) yielding of main reinforcement. The analysis was capable of predicting the two failure modes (a) and (c) described in (2). However, the failure mode (b), the slip along diagonal crack, was not predicted by the analysis. This may be due to the finite element idealization where the shear transfer resistance along the cracks was not assumed correctly, and thus resulting in different stress conditions in the diagonal struts which are vital load carrying member.

ACKNOWLEDGEMENTS

REFERENCES

1. J.Eibl, "Application and Experimental Verification of Advanced Mechanics in Reinforced Concrete", Introductory Report IABSE Colloquium Delft 1981
2. H.Kupfer, H.K.Hilsdorf and H.Rusch, "Behavior of Concrete under Biaxial stresses", ACI Journal, Proceedings Vol. 66, No. 8, August 1969, pp.656-666
3. M.E.Tasuji, A.H.Nilson and F.O.Slate, "Biaxial Stress-Strain relationships for concrete", Magazine of Concrete Research, Vol. 31, No. 109, December 1979, pp217-224
4. H.Onuma and Y.Aoyagi, "Experimental Study on Ultimate Strength and Strain Behavior of Concrete under Biaxial Compressive Stresses, (in Japanese)", Report No.375016, Central Research Institute of Electric Power Industry, July 1976
5. M.D.Kotsovos and J.B.Newman, "A Mathematical description of the deformational behaviour of concrete under complex loading", Magazine of Concrete Research, Vol. 31, No. 107, June 1979, pp77-90